

Feature Analysis for Classification of Physical Actions using surface EMG Data

Anish C. Turlapaty¹ *Member, IEEE* and Balakrishna Gokaraju², *Member, IEEE*

Based on recent health statistics, there are several thousands of people with limb disability and gait disorders that require a medical assistance. A robot assisted rehabilitation therapy can help them recover and return to a normal life. In this scenario, a successful methodology is to use the EMG signal based information to control the support robotics. For this mechanism to function properly, the EMG signal from the muscles has to be sensed and then the biological motor intention has to be decoded and finally the resulting information has to be communicated to the controller of the robot. An accurate detection of the motor intention requires a pattern recognition based categorical identification. Hence in this paper, we propose an improved classification framework by identification of the relevant features that drive the pattern recognition algorithm. Major contributions include a set of modified spectral moment based features and another relevant inter-channel correlation feature that contribute to an improved classification performance. Next, we conducted a sensitivity analysis of the classification algorithm to different EMG channels. Finally, the classifier performance is compared to that of the other state-of-the-art algorithms.

Index Terms—PNN, Feature combinations, classification, sEMG, spectral moments

I. INTRODUCTION

A. Background

THE physical disabilities have been a major problem in the modern world due to various reasons. For example, the aging brings problems such as the gait disorders and limb impairments leading to a loss of the quality of life [1]. Next the occupational, trauma, and sports based injuries and other kind of severe accidents usually render the people either completely or partially disabled. Another major cause of the disabilities in adults is a stroke to the motor cortex or other related regions. For example, an ischemic stroke can lead to motor disabilities, most commonly to the upper limbs [2]. In terms of the statistics, there are 300 amputees per year in the United Kingdom [3] and a total of 185,000 amputees live in the United States [4]. Most of them need a prosthetic limb or a partial limb support. Only a few treatment options are available for these individuals. For instance, a therapeutic rehabilitation can assist the partially disabled people for functional recovery in order to resume normal activities and thus improve the quality of life. In this context, the wearable robots can assist in improving the effectiveness of the rehabilitation [5]. There is a growing evidence that a robot assisted therapy provides an improvement of the motor skills [6], [7]. The key reason for

this improvement is due to the increased therapeutic repetitions and enhanced motivation for the patient due to the involvement of the virtual reality and video gaming [8]. The wearable robotics can also be used to ease the burden on the human beings in various manual tasks. For example, the disabled can be supported by an externally powered prosthetic or an orthotic exoskeleton to restore the limb functionality to some extent [9], [10].

In most of these exoskeleton applications, the key goal is to build a human robot interface that can learn the intention of the user and adapt itself in order to provide an accurate and timely assistance [11]. Note that in a healthy human, there is an active communication between the central nervous system via motor neurons with the concerned muscle groups to produce the intended motion [12]. However, in an amputee or in a person with a stroke induced disability, the bioelectrical signal may not reach the muscles or the muscles may not produce the required force. In these scenarios, an engineering solution is to sense the required myoelectric signal, assuming the signal has a causal relation to the intended motion, using an sEMG sensor on the muscle surface and extract the relevant information. For example, one can estimate the joint force and decode the intended direction needed for the movement and relay it to the controller to generate the intended motion [13], [14]. The sEMG basically refers to the electrical activity associated with the muscles when the muscle fibers are recruited via neuronal firings [15]. A practical exoskeleton product based on surface EMG was invented by an MIT based startup, Myomo, assists people with partial disabilities to perform their daily activities [16]. In this type of research, a major challenge is the design of suitable algorithms and the hardware to cope up with the complexity of human systems and further adapt in an uncertain environment [17]. In the recent years, there is a growing evidence that the pattern recognition (PR) algorithms can be used to learn the motor intention from the surface EMG signals [18]. In the next subsection, we present a survey of the most recent algorithms for PR based control of exoskeletons.

B. Literature Review

This technology usually has two components: (1) an algorithm section that does relevant feature extraction and selection and categorization of movement using a statistical discriminator and (2) a hardware component to interface with an exoskeleton via a controller. In the literature, as discussed below, we find a great deal of emphasis on the algorithm component specifically on the feature extraction. In [12], an online method was developed that has a PR stage and a control mechanism. The classification was performed for 8 hand gestures using

¹ Indian Institute of Information Technology Sri City, Sri City, AP 517646, India. ²The University of West Alabama, Department of CIST, Livingston, AL 35470, USA. Corresponding author: A. Turlapaty email: anish.turlapaty@gmail.com

the RMS value as a feature and a linear SVM achieving 95% accuracy. Next an orthotic arm guided by an EMG based control with upto four degrees of freedom was demonstrated for performing basic manoeuvres in a 3D environment such as simple arm movements, an object pick up and drop and finally a stacking task. In [19], an ANN based control was developed that has sensitivity to the multiple levels of movements of the flexors and the extensors to directly control the orthotic arm. In [14], a PR algorithm was developed to determine the torque level from a human wrist and use it for real time control of an exoskeleton prototype. It was shown that a set of four EMG channels is sufficient for the classification of different wrist actions at different torque levels. In [3], a classification experiment was done, in which three healthy subjects and three amputees participated. The healthy subjects were asked to perform 15 different finger movements and the amputees were asked to imagine 12 different movements. Using the frequency domain features and the SVM, the movements were classified with an accuracy greater than 90%. In [20], the intrinsic mode functions were used for feature extraction toward the classification of six categories of the hand grips. In another work, the cardinality of the EMG signal was proposed as a highly relevant feature for identifying the motor intent [21]. Next, in [4], a classification of six hand grips and finger positions was analysed against the force levels. Nine amputees participated in the study and the key innovation is introduction of the moment ratios as discriminative features for a successful classification with an accuracy over 90% despite discrete variations in the force levels. Next, [22] performed an analysis of the relevant features and the selection of corresponding classifiers for control of the exoskeletons for partially disabled hands. They addressed the classification of sEMG signals corresponding to four hand positions for 20 subjects of which 16 are non-amputees and 4 are partial hand amputees. They have compared the efficiency of the time domain features, the time domain and autoregressive features and the frequency domain features. Next in [23], the local binary pattern based features were used for the classification of the physical action EMG data [24]. A major drawback in [23], is that it is not clear whether the analysis is for a binary classification i.e., the normal vs. the aggressive or for classification of all the 20 categories of the data. In the current paper, we address the above mentioned multi-category classification problem as described in the following sections.

C. Contributions

In our paper, we address the classification of M-categories of physical actions based on multi-channel EMG data. We propose an improved feature set consisting of selected feature subsets from different feature modalities such as the time domain (TD) statistics, the inter-channel TD statistics, the spectral moments ratios and products, the spectral band powers and the local binary pattern based statistics. In the feature extraction apart from other well known features, we have modified the spectral moment features to improve the classification performance. Moreover we have identified an inter-channel correlation feature that also contributes to an improved

classification. Next we present the key EMG channels that significantly contribute toward the performance improvement. Finally, we also demonstrate that the probabilistic neural network classifier has similar performance to that of the kernel based SVM classifier.

II. METHODOLOGY

We consider a dataset \mathbf{X} with $P(= S \times C \times R)$ observation arrays obtained from S subjects. These observations consist of C categories and R trials each i.e., each of the S subjects have performed each activity R times as represented in fig. 1. Finally, each of the p -th observation array X_p has M channels (distinct EMG electrode contact locations) and in each of the m -th channel \mathbf{x}_p^m there are N values (samples).

$$\begin{aligned} \mathbf{X} &= \left\{ X_1, X_2, \dots, X_P \right\} \\ X_p &= \left[\mathbf{x}_p^1, \mathbf{x}_p^2, \dots, \mathbf{x}_p^M \right] \quad p = 1, \dots, P \\ \mathbf{x}_p^m &= \left[x_p^m(1), x_p^m(2), \dots, x_p^m(N) \right]^T \\ & \quad m = 1, \dots, M \end{aligned} \quad (1)$$

The first step is segmentation of the EMG signal in each channel with a non-overlapping and a sliding window length L , which is derived based on the sampling rate of the concerned EMG data. The standard window length (in time) is 200ms from literature, see [14] and [3]. Next, the l -th element of the w -th segment of the m -th channel of the p -th observation is denoted as

$$s_{\mathbf{j}}(l) = x_{\mathbf{j}}((w-1) * L + l) \quad (2)$$

here, \mathbf{j} represents the index triplet $\mathbf{j} = (m, w, p)$, where $w = 1, \dots, N_w$, $l = 1, \dots, L$ and $N_w = \frac{N}{L}$. Note that each pattern can consist of N_s segments and features from each segment are combined to build the complete feature vector corresponding to a pattern.

Now we give an overview of the proposed pattern recognition framework as given in fig. 2. The EMG signals are segmented and the features from various modalities are extracted as described in the subsequent sections. The combined feature set is given as an input to a probabilistic neural network for the classification. Next the relevant features are selected using a forward feature selection algorithm. The performance is analyzed using a 10-fold cross validation. Finally the classification performance is compared with that of a kernel based support vector machines. Next we describe the details of the feature extraction algorithms.

A. Feature Extraction

1) Time Domain Statistics (TDS)

The first subset of features is computed from the sample statistics for each segment within a pattern [25]. The mean value for the \mathbf{j} -th segment (see eq. (2)) is defined as

$$f_t(\mathbf{j}) = \frac{1}{N_w} \sum_{l=1}^{N_w} s_{\mathbf{j}}(l) \quad (3)$$

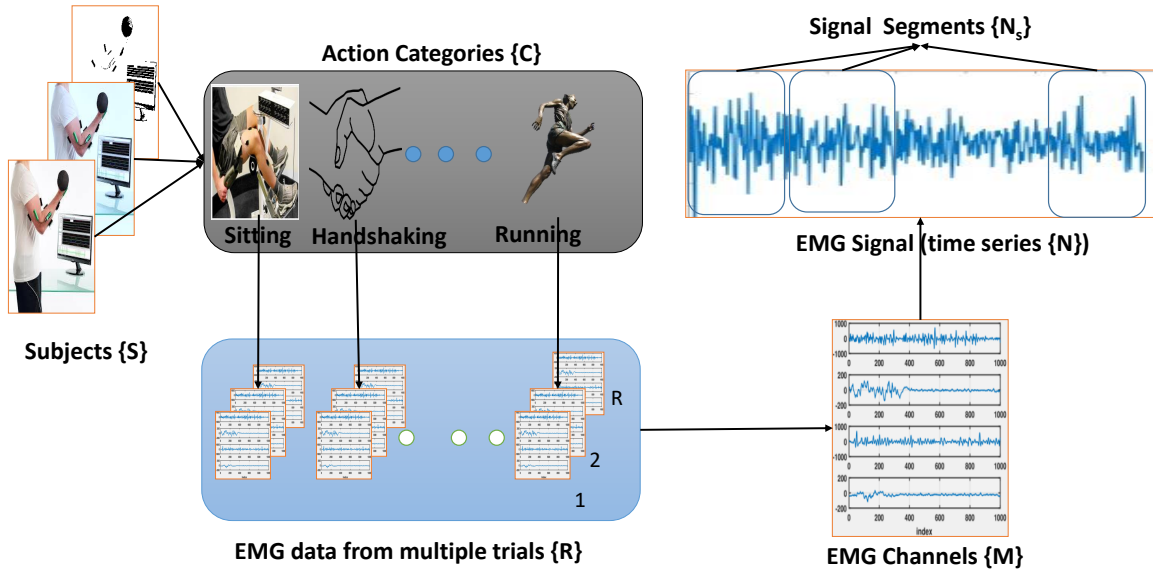


Fig. 1. Physical action data: setup for classification

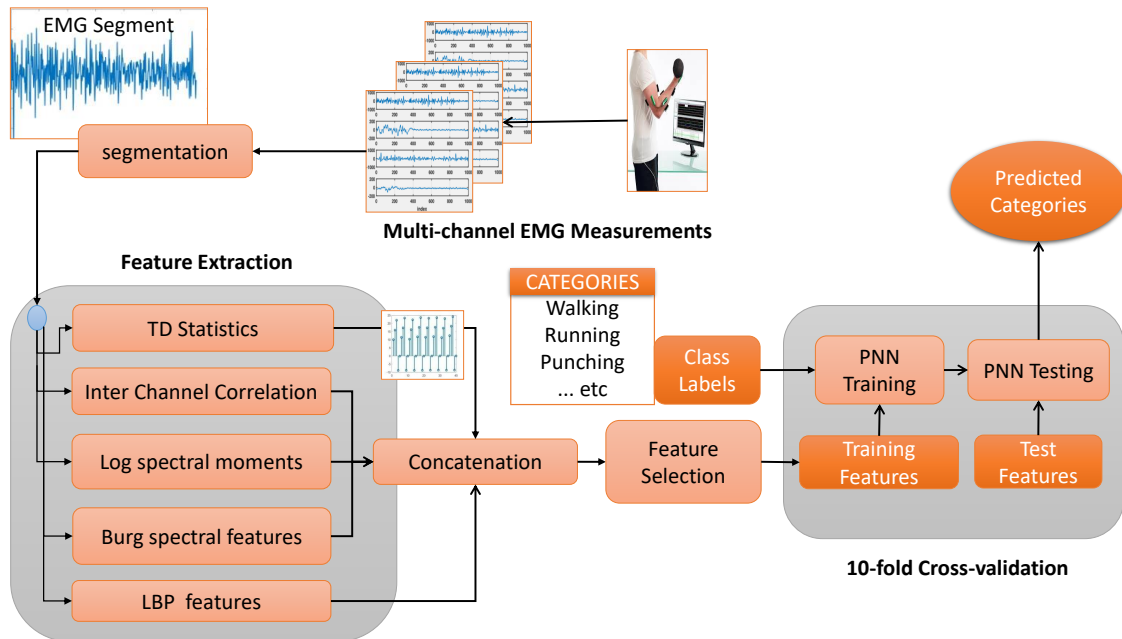


Fig. 2. Physical action data classification scheme using PNN

Similarly, the variance, skewness and kurtosis are computed. Finally, for a p -th pattern, the 4 features from each segment and M channels are grouped into the TDS feature vector.

2) Inter-channel statistics (ICS)

This subset of features is based on maximum cross-correlation [26] among the corresponding w -th segments of the two channels i and j of the p -th signal and is defined as

$$\rho_{w,p}^{i,j} = \max \left(E \{ s_{i,w,p}(l) s_{j,w,p}(l) \} \right) \quad (4)$$

Note that the cross-correlation function need not have a maxima at the zero-lag. Here the values of i and j are chosen from the set C_1 of $\binom{M}{2}$ ordered pairs defined below.

$$C_1 = \{ (i, j) : i = 1, 2, \dots, M-1; \\ j = 2, 3, \dots, M \text{ and } i \neq j \} \quad (5)$$

3) Log Moments of Fourier Spectra (LMF)

The logarithms of moments and their ratios from the frequency domain are computed for the EMG segments based on [3]. Consider the L -point Fourier transform of a segment of the m -th channel of the p -th EMG signal

$$S_j(k) = \sum_{l=1}^L s_j(l) \exp \left(-\frac{j2\pi lk}{L} \right) \quad k = 1, \dots, L \quad (6)$$

Now the squared magnitude spectrum is defined as

$$\psi_j(k) = |S_j(k)|^2 \quad (7)$$

The i -th frequency domain moment from the Fourier transform is defined as [4]

$$g_j(i) = \sqrt{\sum_{k=1}^L k^i \psi_j(k)} \quad (8)$$

where $i \in \{0, \dots, 6\}$. Now, the moment features are defined as

$$\begin{aligned} f_j(1) &= \ln g_j(0) \\ f_j(2) &= \ln g_j(2) \\ f_j(3) &= \ln g_j(4) \\ f_j(4) &= \ln g_j(0) - \frac{1}{2} \ln (g_j(0) - g_j(2)) \\ &\quad - \frac{1}{2} \ln (g_j(0) - g_j(4)) \\ f_j(5) &= \ln g_j(2) - \frac{1}{2} \ln (g_j(0) g_j(4)) \\ f_j(6) &= \ln g_j(0) - \frac{1}{4} \ln (g_j(1) g_j(3)) \\ f_j(7) &= \ln g_j(0) - \frac{1}{4} \ln (g_j(2) g_j(6)) \end{aligned} \quad (9)$$

The pair wise features based on moment products are

$$f_j(n) = \frac{1}{2} \ln g_j(i) g_j(j) \text{ with } n = 8, \dots, 17 \quad (10)$$

where the values of i and j are chosen from the set C_2 of 10 ordered pairs defined below.

$$C_2 = \{ (i, j) : i = 1, 2, 3, 4; j = 2, 3, 4, 5 \text{ and } i \neq j \} \quad (11)$$

Note that the features $f_j(n)$ for $n = 6, \dots, 17$ are newly proposed.

4) Spectral Band Powers (SBP)

The spectral features were previously proposed for the EMG pattern recognition in [27]. In this work, the spectral band power features are extracted as follows. For each channel of the p -th pattern we compute the auto-regression model coefficients $\{a_i\}$ assuming a model of order ν using the Burg's method described in [28].

$$H(\omega_k) = \frac{1}{A(\omega_k)} \quad (12)$$

here $A(\omega)$ is derived from the z-transform $A(z) = \sum_{i=0}^{\nu} a_i z^i$. Next the power spectral density estimate is given by

$$\Psi(\omega_k) = |H(\omega_k)|^2 \sigma_{burg}^2 \quad (13)$$

here σ_{burg}^2 is the error variance computed in the Burg's method. Finally the SBP features are evaluated by dividing the spectrum into N_b bands and computing the respective powers in those bands. For $k = 1, \dots, K_1; K_1 + 1, \dots, K_2; K_2 + 1, \dots, K_3; \dots$, the power within a band is

$$\eta_b = \sum_{k \in b^{th} \text{ band}} \Psi(\omega_k) \quad b = 1, \dots, N_b \quad (14)$$

5) Local Binary Patterns

For the w -th segment of the m -th channel in the p -th pattern, the local binary patterns (LBP) can be computed as follows

$$s_{lbp}(i) = \sum_j \Phi_j^{b(i)} \quad (15)$$

here, Φ_j are the elements of the basis vector used in computing the LBPs for the i -th interval. Next the exponents $b(i)$ are given by

$$b_i = u(\{g_i - g_c\}) \quad (16)$$

here $u(\cdot)$ is the step function and g_i are the values of the signal over a sliding window of length N_{LBP} and g_c is the mean of a subset of the same vector, for details refer to [29]. Finally, the features are computed by counting the number of LBP values above and below a certain threshold τ_{lbp} .

$$\begin{aligned} f_{lbp}^m(1) &= \#\{s_{lbp} \leq \tau_{lbp}\} \\ f_{lbp}^m(2) &= \#\{s_{lbp} > \tau_{lbp}\} \end{aligned} \quad (17)$$

here $\#\{A\}$ represents the cardinality of a set A .

B. Learning using PNN

The application of probabilistic neural networks (PNN) for sEMG signal classification is discussed in [30]. The learning methodology for multi-class problem using the PNN is based on learning the multi-modal multi-variate PDF of the data using the Parzen's method. Ideally, each category has a corresponding mode in the multi-modal pdf. For the test data, the posterior probabilities that a pattern belongs to each of these modes are computed. Next based on maximum among these posterior probabilities, the corresponding class is assigned to the test pattern. The key feature of the PNNs is that there is a separate neuron for each training pattern and hence the size of the network depends on the size of the training data [31].

III. IMPLEMENTATION AND RESULTS

A. Physical Action Dataset

The data set of interest is taken from the UCI Machine learning repository [24]. The dataset consists of the EMG signals recorded using the Delsys EMG electrodes on $S = 4$ subject while they performed $C = 20$ different physical activities of which 10 were aggressive and 10 were normal activities as listed in table I. Each subject repeats the physical action $R = 15$ times. There were 8 EMG electrodes placed on each subject, 4 on biceps and triceps muscle groups of the upper limbs and 4 on the thighs and hamstring muscle groups of the lower limbs. Finally, each channel consists of approximately 10,000 values. Hence, in this study the total sample size becomes $P = 4 \times 20 \times 15 = 1200$.

TABLE I
PHYSICAL ACTION CATEGORIES AND CLASS LABELS

Label	Normal	Label	Aggressive
1	Bowing	11	Elbowing
2	Clapping	12	Frontkicking
3	Handshaking	13	Hammering
4	Hugging	14	Headering
5	Jumping	15	Kneeing
6	Running	16	Pulling
7	Seating	17	Punching
8	Standing	18	Pushing
9	Walking	19	Side-kicking
10	Waving	20	Slapping

B. Application of PNN based classification

The features from $M = 8$ channels for each modality are computed as follows. Based on $R = 15$ and total signal length = 10000, the EMG signal length per trial is $N = 666$. The number segments is $N_s = 1$, and the width $N_w = N$. Next, the feature subsets from the different feature extraction modalities mentioned in section (II-A) are computed and combined into a full feature vector.

$$\mathbf{f}_{all}(p) = [\mathbf{f}_{TDS}(p), \mathbf{f}_{ICS}(p), \mathbf{f}_{LMF}(p), \mathbf{f}_{SBP}(p), \mathbf{f}_{LBP}(p)] \quad (18)$$

As presented in the table II, the cardinality of each subset (except ICS) is $8 \times c_{mod}$, where c_{mod} is the cardinality of the feature subset per modality per channel. For example, for time domain features, the cardinality is $8 \times 4 = 32$.

TABLE II
CARDINALITIES OF EACH FEATURE SUBSET THROUGH COMBINATION OF THE 8 CHANNELS

Feature Subset	TDS	ICS	LMF	SBP	LBP
No. of features	32	12	136	80	16

Now, based on the pairs given in table III, the cross-correlation features (6 each) are computed for the channels from the upper limbs and the lower limbs respectively. The LMF cardinality is based on the fact that each channel has 17 LMF features amounting to a total of 136 features. For the spectral band powers, the number of bands is chosen to be

$N_b = 10$ leading to a total of 80. Finally, the 2 LBP features are computed per channel counting to a total of 12.

TABLE III
CHANNEL PAIRS CONSIDERED FOR COMPUTING THE CROSS-CORRELATION FEATURES

Index	Upper Limbs	Index	Lower Limbs
1	(3,4)	7	(7,8)
2	(2,4)	8	(6,8)
3	(2,3)	9	(6,7)
4	(1,4)	10	(5,8)
5	(1,3)	11	(4,7)
6	(1,2)	12	(5,6)

C. Analysis

In the cross-validation strategy, the sequence of the feature vectors and the output labels is shuffled to avoid any learning bias in the classification. Next the algorithm performance is evaluated by averaging the 10 fold cross-validation based classification accuracies α and kappa accuracies κ across $M_c = 100$ Monte-Carlo runs.

1) Sequential Forward Feature Selection

Now we apply the forward feature selection process to the feature set \mathbf{f}_{all} as follows. The process begins by selecting a feature that has the best accuracy among the individual features. This feature is placed in \mathbf{f}_{sel} , the selected feature subset. In the next step, another performance maximizing feature is selected and added to the same subset \mathbf{f}_{sel} and this process is repeated until the classification performance converges to a maximum. The list of selected features is presented below. The feature index in table IV is based on the cardinality of the subsets given in table II.

TABLE IV
SELECTED FEATURES (INDEX) FROM EACH MODALITY TAKEN FROM THE 8 CHANNELS THAT HAVE SIGNIFICANT CONTRIBUTION TO THE CLASSIFICATION PERFORMANCE

Subsets Channels	TDS	ICS	LMF	SBP	LBP
1	1	6	4, 10, 11, 14, 16	-	-
2	7	3, 6	24, 29, 30, 34	11, 13	-
3	9,10, 11	3	41, 42, 48	23, 26, 30	5
4	-	-	-	31	-
5	17	12	78	-	9
6	23	12	-	-	-
7	25	-	107	66	-
8	29	-	126	-	-

Among the time domain statistics, the mean value of the EMG signal is the key feature selected from the channels 1, 3, 5, 7, 8. Next the variance statistic from the channel 3 is selected. Followed by the skewness from the channels 2, 3 and 6. Finally the kurtosis is not selected and hence irrelevant for improving the classification accuracy.

Next in terms of the inter channel statistics, the correlation between the EMG signals of the channels (1, 2) (i.e., the right biceps and triceps) and (2, 3) (i.e., the right triceps and left biceps), and again the correlation between the channels (5, 6) (i.e., the right thigh and hamstring) have been found to be contributing to the classification (see table V). Next among

TABLE V
CHANNEL PAIRS THAT HAVE SIGNIFICANT CROSS-CORRELATION AND
CONTRIBUTE TO PHYSICAL ACTION CLASSIFICATION

Upper Limbs	Lower Limbs
(1,2); (2,3)	(5,6)

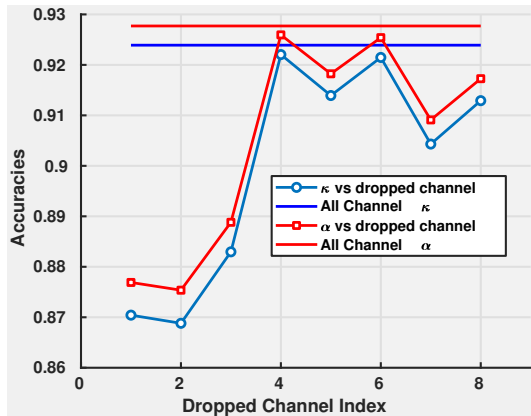


Fig. 3. Sensitivity of classification performance to EMG channels

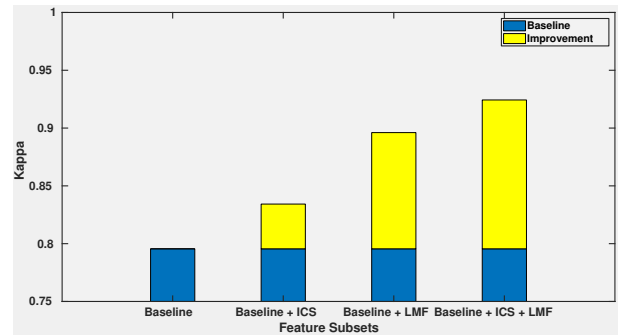
the FFT based moment ratios/products (LMF), the relevant features in each channel are specified in the table IV. Clearly the moment ratio defined as $f_j(7)$ given in eq. 9 is the most relevant feature among the LMF features. Next in the channels 1,2 the moment ratios defined in eq. 10 are found to be of relevance. Next the moment product features $f_j(10)$ in the eq. 10 from the channel 5 and $f_j(5)$ from the channel 7 also contribute to the classification. Finally, among the LMF features, those from the channels 4 and 6 are found to be irrelevant. From the feature selection we note that only the average powers from the bands 2,3,4 and 7 as mentioned in table IV are found to be relevant. Finally, in the case of the local binary patterns based features, the features $f_{lbp}(1)$ from the channels 3,5 and 7 are contributing to the classification.

2) Channel Relevance Analysis

The relevance of the channels toward classification is measured in terms of α and κ . In this approach, we perform the classification of the EMG data, omitting one channel at a time from the selected features as given in table IV, to compute the α and κ . From the $M_c = 100$ runs of each of the 8 cases, we obtain the average classifier performance in a 10-fold cross validation framework and present it in fig. 3. From this figure, it is clear that the channels 1,2 and 3 i.e., the features of the EMG data from the electrodes placed on the right biceps, right triceps and left biceps has the most relevance. Next features corresponding to the channels 7 i.e., left thigh can be ranked second. Finally, the channels 4,5,6 and 8 (left triceps, right thigh, right hamstring and left hamstring) fall third in terms of relevance toward classification.

3) Classification performance and comparisons

The average classification performance when all the feature subsets are used is $\alpha = 93\%$ and $\kappa = 0.925$. Based on only the selected features using the PNN algorithm the average classification accuracy is $\alpha = 92.75\%$ and kappa accuracy $\kappa = 0.924$. The selected features included a few features from



(b)Cohen's Kappa Coefficient κ

Fig. 4. The performance improvement in κ due to inclusion of the proposed and selected features

each subset along with the newly proposed spectral moment ratio and products and the inter channel correlation features. In the fig. 4, the term *Baseline* refers to the subset of 22 selected features that are previously used in existing literature. Next, *ICS* refers to the selected inter-channel correlation features (see table V) and *LMF* refers to the proposed spectral moment ratios and products (see tables IV). As shown in fig 4, the inclusion of the *ICS* features improves the performance by 4%, the *LMF* features improves the kappa performance by 9% and overall improvement due to the proposed features is 11.75%.

The overall performance is given in the confusion matrix in table VI. Recall that the physical actions have two broad categories, the normal and the aggressive. From the confusion matrix in table VI, the first quadrant of the matrix has a significantly stronger diagonal compared to the fourth quadrant which suggests that the PNN classifier is highly successful in learning the normal actions compared to the aggressive actions. The second and the third quadrants are nearly all zeros suggesting that there is very little confusion between the normal and the aggressive activities. In the fourth quadrant, the section of the confusion matrix corresponding to the aggressive activities, shows that there is a slightly higher number of miss-classifications. For example, 16 patterns from the class 19 get classified as the class 12 which means there is a considerable confusion between the front kicking and the side kicking actions. Next, the classification performance of the PNN is compared with that of the multi-class SVM with different kernels. The multi-class SVM is implemented with a $C(C-1)/2$ binary SVM tree using the polynomial kernel. The kappa accuracy $\kappa = 0.91$ and the classification accuracy $\alpha = 91.5\%$. The SVM is implemented with the same set of selected features from the SFS algorithm used in the PNN based approach. A similar feature analysis also applies to the SVM based classification of the physical actions. Finally, there is similar confusion between the front kicking and the side kicking activities, again see the table VII.

TABLE VI
CONFUSION MATRIX FROM PNN WITH 10-FOLD CROSS VALIDATION

Predicted	1	2	3	4	5	6	7	8	9	10	11	12	13	14	15	16	17	18	19	20
True																				
1	58	0	2	0	0	0	0	0	0	0	0	0	0	0	0	0	0	0	0	0
2	0	60	0	0	0	0	0	0	0	0	0	0	0	0	0	0	0	0	0	0
3	0	1	58	0	0	0	0	0	0	1	0	0	0	0	0	0	0	0	0	0
4	0	2	0	58	0	0	0	0	0	0	0	0	0	0	0	0	0	0	0	0
5	0	0	0	0	55	5	0	0	0	0	0	0	0	0	0	0	0	0	0	0
6	0	0	0	0	1	59	0	0	0	0	0	0	0	0	0	0	0	0	0	0
7	0	0	0	0	0	0	59	1	0	0	0	0	0	0	0	0	0	0	0	0
8	0	0	0	0	0	0	3	57	0	0	0	0	0	0	0	0	0	0	0	0
9	0	0	0	0	0	0	0	0	60	0	0	0	0	0	0	0	0	0	0	0
10	0	1	0	0	0	0	0	0	0	59	0	0	0	0	0	0	0	0	0	0
11	0	0	0	0	0	0	0	0	0	0	49	1	2	1	3	0	2	0	0	2
12	0	0	0	0	0	0	0	0	0	0	0	52	2	0	0	0	0	0	4	2
13	0	0	0	0	0	0	0	0	0	0	0	1	56	0	0	0	3	0	0	0
14	0	0	0	0	0	0	0	0	0	0	0	1	0	52	0	0	0	0	0	7
15	0	0	0	0	0	0	0	0	0	0	1	0	0	0	55	2	0	2	0	0
16	0	0	0	0	0	0	0	0	0	1	0	0	0	0	56	1	1	0	0	1
17	0	0	0	0	0	0	0	0	0	0	0	1	0	0	0	59	0	0	0	0
18	0	0	0	0	0	1	0	0	0	0	0	0	0	0	2	4	1	53	0	0
19	0	0	0	0	0	0	0	0	0	0	1	16	0	1	0	0	0	0	41	1
20	0	0	0	0	0	0	0	0	0	0	0	1	0	2	0	0	0	0	0	57

TABLE VII
CONFUSION MATRIX FROM MULTI-CLASS SVM WITH 10-FOLD CROSS VALIDATION

Predicted	1	2	3	4	5	6	7	8	9	10	11	12	13	14	15	16	17	18	19	20
True																				
1	59	0	1	0	0	0	0	0	0	0	0	0	0	0	0	0	0	0	0	0
2	0	58	0	2	0	0	0	0	0	0	0	0	0	0	0	0	0	0	0	0
3	1	0	58	0	0	0	0	0	0	1	0	0	0	0	0	0	0	0	0	0
4	0	1	0	59	0	0	0	0	0	0	0	0	0	0	0	0	0	0	0	0
5	0	0	0	0	58	2	0	0	0	0	0	0	0	0	0	0	0	0	0	0
6	0	0	0	0	3	57	0	0	0	0	0	0	0	0	0	0	0	0	0	0
7	0	0	0	0	0	0	57	3	0	0	0	0	0	0	0	0	0	0	0	0
8	0	0	0	0	0	0	0	59	0	1	0	0	0	0	0	0	0	0	0	0
9	2	0	0	0	0	2	0	0	58	0	0	0	0	0	0	0	0	0	0	0
10	1	1	0	0	0	0	0	0	0	58	0	0	0	0	0	0	0	0	0	0
11	0	0	0	0	0	0	0	0	0	0	57	0	1	1	1	0	0	0	0	0
12	0	0	0	0	0	0	0	0	0	0	0	47	2	0	0	0	0	0	11	0
13	0	0	0	0	0	0	0	0	0	3	0	52	0	0	0	3	2	0	0	0
14	0	0	0	0	0	0	0	0	0	0	0	1	0	53	0	0	0	0	2	4
15	0	0	0	0	0	0	0	0	0	7	4	0	0	48	1	0	0	0	0	0
16	0	0	0	0	0	0	0	0	0	1	0	0	0	1	54	1	2	1	0	0
17	0	0	0	0	0	0	0	0	0	1	0	2	1	0	0	55	1	0	0	0
18	0	0	0	0	0	0	0	0	0	1	0	0	1	1	4	0	49	1	3	0
19	0	0	0	0	0	0	0	0	0	0	9	0	1	0	0	0	0	0	50	0
20	0	0	0	0	0	0	0	0	0	0	0	0	7	0	0	0	0	1	52	0

IV. CONCLUSION

In this study, we have implemented a multi-category classification framework based on the probabilistic neural networks to categorize the physical actions using the features derived from eight channels of the surface EMG data. A set of 276 features were extracted from various modalities including the statistical features in time domain, the inter channel cross correlation features, logarithms of moment ratios of the Fourier spectra, the mean band powers of power spectral density estimates based on the Burg algorithm, and the features based on the local binary patterns. Using the sequential forward selection algorithm a set of 37 features from above 276 features were found to be relevant for the physical action classification. The selected features included a few features from each subset and also a set of modified spectral moment products/ratios and the inter channel correlation features. Based on the selected features using the PNN algorithm, the average classification accuracy is 92.75% and kappa accuracy is 0.924. In terms of channel relevance, the EMG data from the upper limbs has greater significance in physical action classification. Next the classification performance is similar to that of the multi-class SVM (classification 91.5% and the kappa accuracy of 0.91 which requires an extra computational time. The future plans for this research have two important directions. The first is to explore the information theoretic learning methods to improve the classification accuracy and identify a set of relevant features. A second direction is to conduct actual experiments to acquire the EMG measurements for controlling an orthotic exoskeleton for an upper limb. Finally, the overall goal is to find an optimal combination of learning algorithms and control strategies for the upper limb exoskeletons.

REFERENCES

- [1] H. Stolze, S. Klebe, C. Baecker, C. Zechlin, L. Friege, S. Pohle, and G. Deuschl, "Prevalence of gait disorders in hospitalized neurological patients," *Movement disorders*, vol. 20, no. 1, pp. 89–94, 2005.
- [2] T. Proietti, V. Crocher, A. Roby-Brami, and N. Jarrasse, "Upper-limb robotic exoskeletons for neurorehabilitation: A review on control strategies," *IEEE Reviews in Biomedical Engineering*, vol. 9, pp. 4–14, 2016.
- [3] A. H. Al-Timemy, G. Bugmann, J. Escudero, and N. Outram, "Classification of finger movements for the dexterous hand prosthesis control with surface electromyography," *IEEE Journal of Biomedical and Health Informatics*, vol. 17, no. 3, pp. 608–618, 2013.
- [4] A. H. Al-Timemy, R. N. Khushaba, G. Bugmann, and J. Escudero, "Improving the Performance Against Force Variation of EMG Controlled Multifunctional Upper-Limb Prostheses for Transradial Amputees," *IEEE Transactions on Neural Systems and Rehabilitation Engineering*, vol. 24, no. 6, pp. 650–661, 2016.
- [5] A. C. Lo, P. D. Guarino, L. G. Richards, J. K. Haselkorn, G. F. Wittenberg, D. G. Federman, R. J. Ringer, T. H. Wagner, H. I. Krebs, B. T. Volpe *et al.*, "Robot-assisted therapy for long-term upper-limb impairment after stroke," *New England Journal of Medicine*, vol. 362, no. 19, pp. 1772–1783, 2010.
- [6] N. Jarrasse, T. Proietti, V. Crocher, J. Robertson, A. Sahbani, G. Morel, and A. Roby-Brami, "Robotic exoskeletons: a perspective for the rehabilitation of arm coordination in stroke patients," *Frontiers in human neuroscience*, vol. 8, p. 947, 2014.
- [7] V. Grosu, C. R. Guerrero, B. Brackx, S. Grosu, B. Vanderborght, and D. Lefeber, "Instrumenting complex exoskeletons for improved human-robot interaction," *IEEE Instrumentation and Measurement Magazine*, vol. 18, no. 5, pp. 5–10, 2015.
- [8] P. S. Lum, C. G. Burgar, P. C. Shor, M. Majmundar, and M. Van der Loos, "Robot-assisted movement training compared with conventional therapy techniques for the rehabilitation of upper-limb motor function after stroke," *Archives of Physical Medicine and Rehabilitation*, vol. 83, no. 7, pp. 952–959, 2002.
- [9] S. Benatti, B. Milosevic, E. Farella, E. Gruppioni, and L. Benini, "A Prosthetic Hand Body Area Controller Based on Efficient Pattern Recognition Control Strategies," *Sensors*, vol. 17, no. 4, p. 869, 2017.
- [10] H. Kazerooni, A. Chu, and R. Steger, "That which does not stabilize, will only make us stronger," *International Journal of Robotics Research*, vol. 26, no. 1, pp. 75–89, 2007.
- [11] J. Rosen, M. Brand, M. B. Fuchs, and M. Arcan, "A myosignal-based powered exoskeleton system," *IEEE Transactions on systems, Man, and Cybernetics-part A: Systems and humans*, vol. 31, no. 3, pp. 210–222, 2001.
- [12] P. Shenoy, K. J. Miller, B. Crawford, and R. P. Rao, "Online electromyographic control of a robotic prosthesis," *IEEE Transactions on Biomedical Engineering*, vol. 55, no. 3, pp. 1128–1135, 2008.
- [13] T. Lenzi, S. M. M. De Rossi, N. Vitiello, and M. C. Carrozza, "Intention-based EMG control for powered exoskeletons," *IEEE Transactions on Biomedical Engineering*, vol. 59, no. 8, pp. 2180–2190, 2012.
- [14] Z. O. Khokhar, Z. G. Xiao, and C. Menon, "Surface EMG pattern recognition for real-time control of a wrist exoskeleton," *BioMedical Engineering Online*, vol. 9, p. 41, 2010.
- [15] C. J. de Luca, "Physiology and Mathematics of Myoelectric Signals," *IEEE Transactions on Biomedical Engineering*, vol. BME-26, no. 6, pp. 313–325, 1979.
- [16] L. M. Vaca Benitez, M. Tabie, N. Will, S. Schmidt, M. Jordan, and E. A. Kirchner, "Exoskeleton technology in rehabilitation: Towards an EMG-based orthosis system for upper limb neuromotor rehabilitation," *Journal of Robotics*, vol. 2013, p. 13, 2013.
- [17] E. Scheme and K. Englehart, "Electromyogram pattern recognition for control of powered upper-limb prostheses: State of the art and challenges for clinical use," *Journal of Rehabilitation Research and Development*, vol. 48, no. 6, pp. 643–660, 2011.
- [18] M. Khezri and M. Jahed, "Real-time intelligent pattern recognition algorithm for surface EMG signals," *BioMedical Engineering Online*, vol. 6, p. 45, 2007.
- [19] T. Tsuji, K. Shima, N. Bu, and O. Fukuda, "Biomimetic impedance control of an emg-based robotic hand," in *Robot Manipulators Trends and Development*. Rijeka: InTechOpen, 2010, ch. 9.
- [20] C. Sapsanis, G. Georgoulas, and A. Tzes, "EMG based classification of basic hand movements based on time frequency features," in *2013 21st Mediterranean Conference on Control and Automation, MED 2013 - Conference Proceedings*, 2013, pp. 716–722.
- [21] M. Ortiz-Catalan, "Cardinality as a highly descriptive feature in myoelectric pattern recognition for decoding motor volition," *Frontiers in neuroscience*, vol. 9, p. 416, 2015.
- [22] A. A. Adewuyi, L. J. Hargrove, and T. A. Kuiken, "Evaluating EMG Feature and Classifier Selection for Application to Partial-Hand Prosthesis Control," *Frontiers in Neurobotics*, vol. 10, p. 15, 2016.
- [23] Ö. F. Erturul, Y. Kaya, and R. Tekin, "A novel approach for SEMG signal classification with adaptive local binary patterns," *Medical & Biological Engineering & Computing*, pp. 1137–1146, 2015.
- [24] M. Lichman, "UCI machine learning repository," 2013. [Online]. Available: <http://archive.ics.uci.edu/ml>
- [25] B. Hudgins, P. Parker, and R. N. Scott, "A new strategy for multifunction myoelectric control," *IEEE Transactions on Biomedical Engineering*, vol. 40, no. 1, pp. 82–94, 1993.
- [26] L. H. Smith and L. J. Hargrove, "Comparison of surface and intramuscular emg pattern recognition for simultaneous wrist/hand motion classification," in *Engineering in Medicine and Biology Society (EMBC), 2013 35th Annual International Conference of the IEEE*. IEEE, 2013, pp. 4223–4226.
- [27] R. N. Khushaba, M. Takruri, J. V. Miro, and S. Kodagoda, "Towards limb position invariant myoelectric pattern recognition using time-dependent spectral features," *Neural Networks*, vol. 55, pp. 42–58, 2014.
- [28] P. Stoica and R. Moses, *Spectral analysis of signals*. Upper Saddle River, New Jersey: Pearson, 2005.
- [29] T. Mäenpää, *The local binary pattern approach to texture analysis—extensions and applications*. Oulun yliopisto Oulu, 2003.
- [30] N. Bu, M. Okamoto, and T. Tsuji, "A hybrid motion classification approach for emg-based human–robot interfaces using bayesian and neural networks," *IEEE Transactions on Robotics*, vol. 25, no. 3, pp. 502–511, 2009.
- [31] D. F. Specht, "Probabilistic neural networks," *Neural Networks*, vol. 3, no. 1, pp. 109–118, 1990.